Amorphous-amorphous transition and the two-step replica symmetry breaking phase

Andrea Crisanti[1,*] and Luca Leuzzi[1,2,†]
[1]*Dipartimento di Fisica, Università di Roma "La Sapienza," P.le Aldo Moro 2, I-00185 Roma, Italy*
[2]*Statistical Mechanics and Complexity Center (SMC), INFM, CNR, Rome, Italy*
(Received 23 August 2007; published 15 November 2007)

The nature of polyamorphism and amorphous-to-amorphous transitions is investigated by means of an exactly solvable model with quenched disorder, the spherical $s+p$ multispin interaction model. The analysis is carried out in the framework of replica symmetry breaking theory and leads to the identification of low-temperature glass phases of different kinds. Besides the usual one-step solution, known to reproduce all basic properties of structural glasses, also a physically consistent two-step solution arises. More complicated phases are found as well, as temperature is further decreased, expressing a complex variety of metastable-state structures for amorphous systems.

DOI: 10.1103/PhysRevB.76.184417 PACS number(s): 75.10.Nr, 05.50.+q, 11.30.Pb

I. INTRODUCTION

In recent years increasing evidence has been collected for the existence of amorphous to amorphous transitions (AATs), in various glass-forming substances such as, e.g., vitreous germania and silica, where the coordination changes abruptly under pressure shifts.[1] One refers to this phenomenon as "polyamorphism."[1,2] Like the liquid-glass transition also the AAT is not a thermodynamic phase transition, but it amounts to a qualitative change in the relaxation dynamics, apparently expressing a recombination of the glass structure. Other kinds of AATs are known to occur, e.g., in porous silicon,[3] in undercooled water,[4,5] in copolymer micellar systems,[6] and in polycarbonate and polystyrene glassy polymers.[7]

A number of theoretical models have been introduced to describe systems undergoing AATs, such as, e.g., a model of hard-core repulsive colloidal particles subject to a short-range attractive potential.[8–10] Another instance is the spherical p-spin model on a lattice gas of Ref. 11. In this paper we consider a model with multibody quenched disordered interactions where various AATs occur as well: the spherical $(s+p)$-spin model.

Our analytic investigation is performed by applying Parisi's replica symmetry breaking (RSB) theory.[12] In the framework of the theoretical description of glasses and, more generally, of disordered systems, RSB theory provides, in a broad variety of instances, a rather deep and complex mean-field insight. RSB solutions so far encountered, representing physically stable phases, are either one-step RSB (mean-field glass) or implement a continuous hierarchy of breakings (mean-field *spin* glass). One-step RSB (1RSB) solutions are, e.g., found in the Ising p-spin[13,14] and Potts[15] models with quenched disorder in a low-temperature interval[16] or in the spherical p-spin model below the static critical temperature,[17] else in optimization problems mapped onto dilute spin-glass systems such as the XOR-SAT (where it correctly describes the whole UNSAT phase),[18] or the K-SAT, with $K>2$,[19] in a certain interval of connectivity values next to the SAT-UNSAT transition.[20] The continuous, or *full* RSB (FRSB) solution describes, instead, the low-temperature phase of the mean-field version of the Ising spin glass—i.e., the Sherrington-Kirkpatrick model.[21] Low-temperature phases with a continuous hierarchy of states are known to exist also for other disordered models with discrete variables, such as the above-mentioned Ising p-spin and Potts models, even though these might display a further discontinuous RSB step.[22] A purely FRSB phase has been, eventually, found in a model with continuous variables, constituted by a two-body and a p-body interaction term: the spherical $(2+p)$-spin model.[24,25]

In the present work we consider the spherical $(s+p)$-spin model with both s and $p>2$, addressing physically consistent RSB solutions qualitatively different from those mentioned above (also different from the $s=2$ model case). The Hamiltonian of the model is

$$\mathcal{H}=\sum_{i_1<\cdots<i_s} J^{(s)}_{i_1,\ldots,i_s}\sigma_{i_1}\cdots\sigma_{i_s}+\sum_{i_1<\cdots<i_p} J^{(p)}_{i_1,\ldots,i_p}\sigma_{i_1}\cdots\sigma_{i_p}, \tag{1}$$

where $J^{(t)}_{i_1,\ldots,i_t}$ $(t=s,p)$ are uncorrelated, zero-mean, Gaussian variables of variance

$$\overline{(J^{(t)}_{i_1\cdots i_t})^2}=\frac{J_t^2 t!}{2N^{t-1}},\quad i_1<\cdots<i_t, \tag{2}$$

and σ_i are N continuous variables obeying the spherical constraint $\Sigma_i\sigma_i^2=N$. Equation (1) is clearly symmetric in s and p. We will always consider $p>s$. The properties of the model strongly depend on the value of s and p: for $s=2$, $p=3$ the model reduces to the spherical p-spin model in a field[17] with a low-temperature 1RSB phase, while for $s=2$, $p\geqslant 4$ the model posses an additional FRSB low-temperature phase[24,26] and a 1-FRSB phase.[25] For $s,p>2$ the phases displayed are the paramagnet and the 1RSB spin glass, as far as the difference $p-s$ is not too large.[25] Recently, Krakoviack observed that for large $p-s$ more than a simple paramagnet-1RSB transition is likely to occur.[27]

The dynamic equations of the $s+p$ model can be formally rewritten as mode coupling theory (MCT) equations in the *schematic* approximations (see, e.g., Refs. 28–31), and defining the auxiliary thermodynamic parameters $\mu_t=t\beta^2J_t^2/2$, a mapping can be established with the binomial schematic theories $F_{s-1,p-1}$ with a scalar kernel (see, e.g., Ref. 32). In

particular, the F_{13} theory studied by Götze and Sjögren[29] is dynamically equivalent to a 2+4 spherical spin model.[33]

II. LARGE $p-s$ SPHERICAL $(s+p)$-SPIN MODEL

Analyzing the model for $s>2$ and large $p-s$, we observe a very rich phase diagram even though no purely continuous FRSB phase, as obtained in the $(2+p)$-spin model,[24,25] is encountered in the present case. We now concentrate on the static scenario.

The static free energy functional reads, for a generic number R of RSBs, as[25]

$$-\beta\Phi = \frac{1}{2}(1+\ln 2\pi) + \lim_{n\to 0}\frac{1}{n}G[\mathbf{q}], \tag{3}$$

$$2G[\mathbf{q}] = \sum_{ab}^{1,n} g(q_{ab}) + \ln\det \mathbf{q}, \tag{4}$$

where

$$g(q) = \frac{\mu_s}{s}q^s + \frac{\mu_p}{p}q^p \tag{5}$$

and $\mathbf{q}=\{q_{ab}\}$ is the Parisi overlap matrix taking values $0=q_0<q_1<\cdots<q_R<q_{R+1}=1$. In the absence of an external field, $q_0=0$. For any R, $G[\mathbf{q}]$ can be written as

$$\frac{2}{n}G[\mathbf{q}] = \int_0^1 dq x(q)\Lambda(q) + \int_0^{q_R}\frac{dq}{\chi(q)} + \ln(1-q_R), \tag{6}$$

where

$$x(q) = p_0 + \sum_{r=0}^{R}(p_{r+1}-p_r)\theta(q-q_r) \tag{7}$$

is the cumulative probability density of the overlaps,

$$\Lambda(q) = \frac{dg(q)}{dq} \tag{8}$$

and

$$\chi(q) = \int_q^1 dq' x(q'). \tag{9}$$

Stationarity of Φ with respect to q_r and p_r leads, respectively, to the self-consistency equations

$$\mathcal{F}(q_r) = 0, \quad r=0,\ldots,R, \tag{10}$$

$$\int_{q_{r-1}}^{q_r} dq\mathcal{F}(q) = 0, \quad r=1,\ldots,R, \tag{11}$$

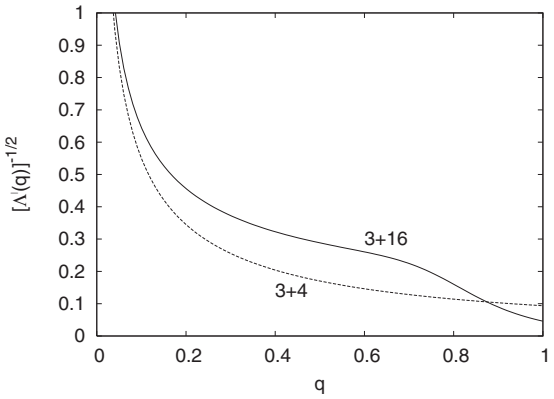

FIG. 1. Right-hand side of Eq. (13) for $\mu_s=12$ and $\mu_p=30$. The $s+p=3+4$ curve (dotted line) can have no more than two intersections with $\chi(q)$, implying at most a 1RSB solution. This shape is independent of the particular values of the μ's [see Eq. (15) and discussion thereafter]. For $s=3$ and $p=16$ (solid curve) there is, instead, evidence for the existence of a maximum of four intersections with the concave $\chi(q)$ (because of the double change of convexity), yielding a 2RSB solution. This does not occur in the entire plane but only in a subregion. In the q interval of negative convexity of $[\Lambda'(q)]^{-1/2}$, $\chi(q)$ can also overlap the curve in a continuous interval, yielding, furthermore, continuous RSB solutions.

where

$$\mathcal{F}(q_r) \equiv \Lambda(q_r) - \int_0^{q_r}\frac{dq}{\chi(q)^2}. \tag{12}$$

Equation (11) implies that $\mathcal{F}(q)$ has at least one root in each interval $[q_{r-1},q_r]$, which, by the way, is not a solution of the whole set of self-consistency equations.

III. HOW MANY RSBs?

Which kind of solutions are physically consistent for the model at large $p-s$? Following Refs. 17 and 25, we observe that Eqs. (10) and (11) guarantee that between any pair $[q_{r-1},q_r]$ there must be at least two extremes of $\mathcal{F}$ (we recall that here $q_0=0$). Denoting the extremes by q^*, the condition $\mathcal{F}'(q^*)=0$ leads to the equation

$$\chi(q^\star) \equiv \int_{q^\star}^1 x(q)dq = \frac{1}{\sqrt{\Lambda'(q^\star)}}, \tag{13}$$

where

$$\Lambda'(q) = \frac{d\Lambda(q)}{dq} = (s-1)\mu_s q^{s-2} + (p-1)\mu_p q^{p-2}. \tag{14}$$

Since $x(q)$ is a nondecreasing function of q, $\chi(q)$ has a negative convexity. The convexity of the function $[\Lambda'(q)]^{-1/2}$ depends, instead, on s and p, as well as on the parameters μ_s and μ_p. If $p-s$ is not too large, it displays a positive convexity in the whole (μ_p,μ_s) plane, whereas, as p is larger than some critical value that depends on s, the curve can, actually, change convexity in a certain region of the (μ_p,μ_s) plane.

The right-hand side of Eq. (13) is plotted in Fig. 1 in two

qualitatively different model cases with $p>s>2$. For nearby values of s and p (dashed curve, $s=3$, $p=4$) the shape of $[\Lambda'(q)]^{-1/2}$ implies that at most a 1RSB solution can take place. When $p-s$ grows, however, the qualitative behavior changes (solid curve, $s=3$, $p=16$) and the 1RSB is no longer the only solution admissible: solutions with more RSBs may occur in order to stabilize the system. From Fig. 1 one can readily see that for certain values of μ_s and μ_p, and large $p-s$, Eq. (13) can have four solutions; i.e., $\mathcal{F}(q)$ can display four extremes, allowing for the existence of a 2RSB phase. The critical values of p for fixed $s>2$, above which this kind of phase can show up, are those at which the $[\Lambda'(q)]^{-1/2}$ function acquires a negative convexity at some given q value between 0 and 1—i.e., the values for which

$$(p^2+p+s^2+s-3sp)^2-ps(p-2)(s-2)=0, \qquad (15)$$

e.g., $(s,p)=(3,8)$, $(4,7+2\sqrt{6})$, $(5,9+3\sqrt{5})$. As s increases, the relative critical p becomes very large.[34] Notice that Eq. (15) does not depend on the parameters μ. For $p(s)$ less than the root of the equation, $[\Lambda'(q)]^{-1/2}$ has always a positive convexity (see the 3+4 curve in Fig. 1), while for larger values of p its convexity can be negative for some range of values of the μ's.

Equations (10) and (11) also admit continuous RSB solutions ($q_r-q_{r-1}\to 0$). They reduce to the same identity in this case, as well as $\mathcal{F}'(q)=0$ [Eq. (13)]. The latter sets a constraint on the interval of q values over which a FRSB ansatz can be constructed because Eq. (13) can only hold as far as $[\Lambda'(q)]^{-1/2}$ has the same (negative) convexity as $\chi(q)$. A continuous RSB structure in a certain interval of q values does not rule out, however, the possibility of discrete RSBs in other intervals. Indeed, "mixed" solutions are found as well, whose overlap function $q(x)$ the inverse of $x(q)$ display both discontinuous steps and a continuous part.

IV. PHASE DIAGRAM

We now inspect the explicit case where $s=3$ and $p=16$, which is enough to catch the properties that make the model special, without loss of generality. The complete phase diagram is plotted in the MCT-like variables μ_3 and μ_{16} in Fig. 2, where we only report the static transition lines. We stress, however, that all static transitions have a dynamic counterpart, as we will discuss in a later section. In each phase, the shape of the overlap function $q(x)$ is sketched. Going clockwise, in the central part we identify a paramagnetic (PM) phase, a 1RSB glassy phase (I), a 2RSB glassy phase, and a second 1RSB phase (II). Even though the structure of the states organization is qualitatively similar, the two 1RSB phases differ in the value of the self-overlap q_1 (or Edwards-Anderson parameter[35]) and the position p_1 of the RSB step along the x axis. In the top part of the phase diagram things get even more diversified, and we find the additional mixed continuous-discontinuous "F-1RSB" (shaped as in the top-left inset of Fig. 2) (Ref. 36) and "1-F-1RSB" phases.

In Fig. 3 a detail of the phase diagram is plotted around the quadricritical point where four transition lines meet. We use in this case the natural thermodynamic parameters T and

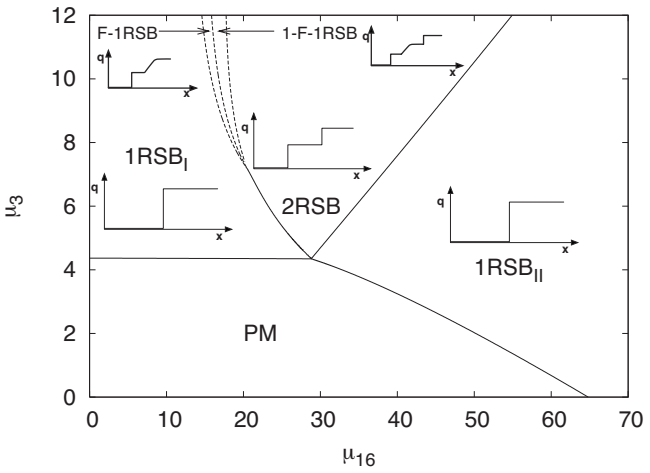

FIG. 2. Static (μ_p,μ_s) phase diagram of the spherical 3+16 spin glass model. PM: Paramagnetic phase; 1(2)RSB: one (two) step(s) RSB phase; F-1RSB: full RSB with one discontinuous step at low q: 1-F-1RSB; full RSB terminating both with a step at small and large q. Overlap order parameter functions are drawn in the various phases.

J_p (in units of J_s) rather than the MCT parameters μ_s and μ_p. The dynamic transition curves are also plotted (dashed lines) in this case. We notice that decreasing the temperature the dynamic transition always takes place before the static one.

Starting in the 1RSB$_I$ phase for low values of the ratio J_p/J_s, if we increase J_p keeping the temperature fixed, at some point A (see Fig. 4) a 2RSB phase arises with the same free energy of the 1RSB$_I$. As J_p is further increased, the 2RSB phase displays a higher free energy than the 1RSB$_I$ one (bottom inset of Fig. 4). Since we are considering replicated objects in the limit of the number of replicas going to zero, this implies that the 2RSB phase is the stable one, whereas the 1RSB phase becomes metastable. In Fig. 4 we show the detail of the 1RSB$_I$-2RSB-1RSB$_{II}$ isothermal transitions in J_p/J_s. In the inset we show the free energies $\Phi(T/J_s,J_p/J_s)$ relative to each phase. It is clear that, were the 2RSB phase not there, a coexistence region would occur, as

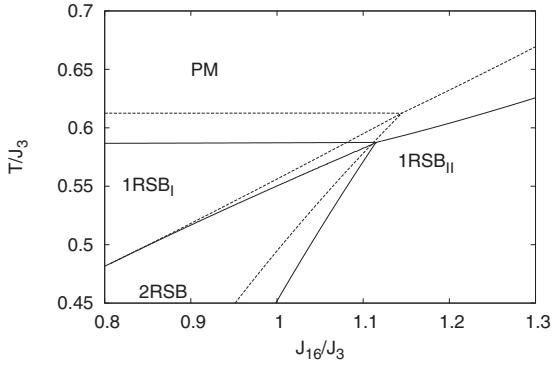

FIG. 3. Detail of the T-J_{16} phase diagram around the static (solid line) and dynamic (dashed line) quadricritical points. Temperature and J_{16} are in units of J_3. Starting from any phase in the diagram lowering the temperature the system first undergoes the dynamic transition and then the statics.

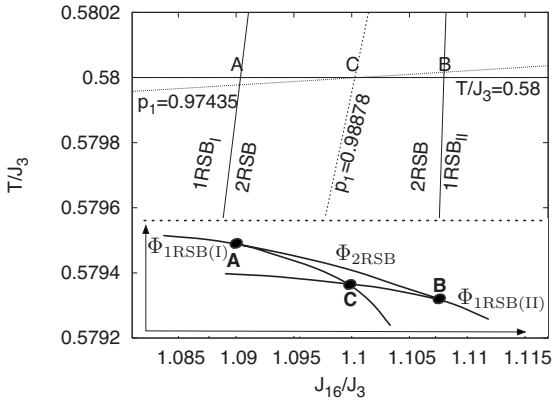

FIG. 4. Phase transitions at fixed $T=0.58$ varying J_{16} in J_3 units. Point C is the (avoided) first-order phase transition, A and B 1RSB/2RSB transition points. Bottom: qualitative picture of the behavior of the isothermal free energy versus J_{16}. As J_{16} is increased the globally stable thermodynamic phase passes from a 1RSB to a 2RSB solution and back to a 1RSB one.

well as a related first-order $1\mathrm{RSB}_I$-$1\mathrm{RSB}_{II}$ phase transition (point C). The rising of the 2RSB phase covering the whole interested region, however, prevents the occurrence of a first-order phase transition.

In terms of state reorganization, or order parameter functional shape, the way the system undergoes the $1\mathrm{RSB}_I$-2RSB and 2RSB-$1\mathrm{RSB}_{II}$ transitions is not the same, as is reported in Fig. 5. The first transition is a straightforward generalization of the p-spin-model PM-1RSB transition (also taking place in the present model; see Figs. 2 and 3): the second step appears, indeed, at $x=1$ as the highest one. This means that new states arise *inside* the states of the 1RSB phase, while the latter acquire the status of clusters of states. We will refer to this kind of transition as *state fragmentation*.[37] Across the second kind of transition, instead, going from the $1\mathrm{RSB}_{II}$ to the 2RSB phase, an intermediate step of $q(x)$ appears at p_1. This corresponds to grouping the states into clusters whose relative overlap is equal to the value of the intermediate step—between p_2 and p_1 in the right-hand-side (rhs) overlap picture in Fig. 5—i.e., the system undergoes a sort of *state clustering* transition. Precursory symptoms of these transitions were observed in a glassy model on Bethe lattice in Ref. 37 where the 1RSB solution of the model proved unstable in the close packing limit and two kinds of instability were considered, leading to the onset of a phase described by a more refined RSB ansatz. Here we have an explicit realization of that conjecture.

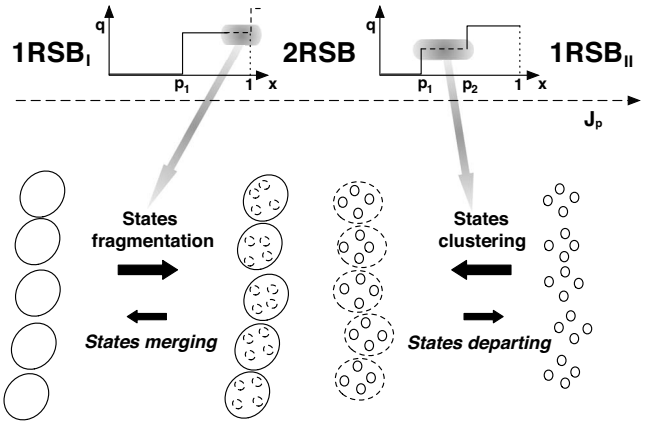

FIG. 5. Qualitative change of the overlap function across the $1\mathrm{RSB}_I$-2RSB and 2RSB-$1\mathrm{RSB}_{II}$ transitions. The first transition occurs as a second step at larger q appears at $p_2=1$. The second one takes place as the intermediate step between p_1 and p_2 shrinks and vanishes.

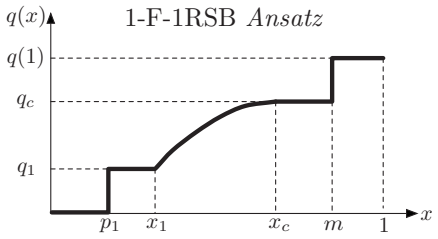

FIG. 6. Picture of the 1-F-1RSB solution and relative notation for the overlap values (q axis) and the replica symmetry breaking parameter values (x axis).

A. Formal characterization of phases and transitions

In order to describe the various phases and their relative transitions, one has to solve the saddle point equations (10) and (11). In introducing the RSB solutions describing the frozen phases of the spherical $s+p$ model for large $p-s$, we start from the most complicated one that we have found: the 1-F-1RSB phase. From the equations describing this one, indeed, the self-consistency equations of all other phases can be straightforwardly derived, as well as the phase transition lines.

In general, we will denote by q_1 the value of the first step in the overlap function $q(x)$ and by p_1 its position on the x axis. The last step will be identified by $q(1)$—i.e., the value of $q(x)$ in $x=1$—and the relative step position by m. If a continuous part is present, we call its highest overlap value q_c, reached at $x_c=x(q_c)$. The initial point on the x axis of the continuous part is $x_1=x(q_1)$. In Fig. 6 a pictorial plot of the 1-F-1RSB $q(x)$ is shown, to help fix the notation.

The self-consistency equations [cf. Eq. (10)] are expressed, for this solution, by

$$\Lambda(q(1)) - \Lambda(q_c) = \frac{q(1) - q_c}{\chi(q(1))\chi(q_c)}, \tag{16}$$

$$\Lambda(q) - \Lambda(q_1) = \int_{q_1}^{q} \frac{dq}{\chi^2(q)}, \quad q_1 \leqslant q \leqslant q_c, \tag{17}$$

$$\Lambda(q_1) = \frac{q_1}{\chi(0)\chi(q_1)}, \tag{18}$$

where $\chi(q)$ is given in Eq. (9) and in the above cases (no external field, $q_0=0$) it takes the expressions

$$\chi(q(1)) = 1 - q(1), \tag{19}$$

$$\chi(q_c) = 1 - q(1) + m[q(1) - q_c], \tag{20}$$

$$\chi(q_1) = 1 - q(1) + m[q(1) - q_c] + \int_{q_1}^{q_c} dq x(q), \tag{21}$$

$$\chi(0) = 1 - q(1) + m[q(1) - q_c] + \int_{q_1}^{q_c} dq x(q) + p_1 q_1. \tag{22}$$

Using the function

$$z(y) = -2y\frac{1 - y + \ln y}{(1-y)^2} \tag{23}$$

introduced by Crisanti and Sommers (CS) in Ref. 17, the self-consistency equation for the RSB points p_1 and m [cf. Eq. (11)] become

$$z(y(1)) = 2\frac{g(q(1)) - g(q_c) - [q(1) - q_c]\Lambda(q_c)}{[q(1) - q_c][\Lambda(q(1)) - \Lambda(q_c)]}, \tag{24}$$

$$z(y_1) = 2\frac{g(q_1)}{q_1 \Lambda(q_1)}, \tag{25}$$

with

$$y_1 = \frac{\chi(q_1)}{\chi(0)}, \quad y(1) = \frac{\chi(q(1))}{\chi(q_c)}. \tag{26}$$

From this phase the system can undergo two transitions: toward a F-1RSB phase, on the left-hand side in the (μ_{16}, μ_3) plane, and toward a 2RSB phase, on the right hand-side (see Fig. 2). Transforming into the 2RSB phase, $q_c \to q_1$ and the continuous part disappears. The saddle point equations left to yield the solution are Eqs. (16) and (24), with $q_c = q_1$, together with Eqs. (18) and (25). We might say that we are facing a state *departing*—i.e., the opposite of the state clustering mentioned in the previous section and on the rhs of Fig. 5. This, now, takes place on a continuous set of ultrametric levels, eliminating the whole intermediate structure of clusters of clusters, and eventually leaves a three-level organization. On the left-hand side, instead, the F-1RSB/1-F-1RSB transition occurs as $q(1) = q_c$ and Eqs. (16) and (24) become trivial identities. Coming from the F-1RSB side, states break down into smaller states, themselves becoming clusters of these newborn states. This is a fragmentation transition (cf. lhs of Fig. 5) and Ref. 37.

We now continue scanning the phase diagram of Fig. 2 counterclockwise. Decreasing the variances of the random coupling distribution at constant temperature, or else increasing the temperature at fixed interaction variances, the system in the F-1RSB phase ends up in a 1RSB frozen phase. At the transition $q_c \to q_1$ and the continuous part is suppressed.[38] The whole ultrametric continuous structure inside the largest clusters merges into simple states.

Lowering μ_3 (i.e., increasing the temperature or decreasing J_3) the system reaches the paramagnetic phase at which q_1 jumps to 0 discontinuously, because p_1 overcomes 1, and only one state remains. Increasing μ_{16}, the paramagnet goes back to a frozen—multistate—glassy phase, the 1RSB_{II}, as a step q_1 appears at $x = p_1 = 1$. These last two are transitions of the kind occurring in the spherical p-spin model in which the Edwards-Anderson order parameter discontinuously jumps from zero to q_1. They are also termed random first order transitions.[39]

From the 1RSB_{II} phase the system goes into a 2RSB phase in a state clustering transition, as already mentioned above and shown in Fig. 5 (right-hand side). Eventually, from the 2RSB the system can transform into the 1RSB_I phase (left-hand side of Fig. 5) or into our starting phase, the 1-F-1RSB phase.

V. DYNAMIC TRANSITIONS

For what concerns the dynamic glass transitions (dashed lines in Fig. 3), they can be obtained looking at the dynamical solutions as formulated in Ref. 33, where the equilibrium dynamics of the system in the different regions of the parameters space was analyzed and the solution for a generic number of different relaxation times was provided. In the dynamic-static analogy initially proposed by Sompolinsky,[40] each of the relaxation time bifurcations corresponds to a RSB. The dynamic solution equivalent to the static 1-F-1RSB phase is described by Eqs. (16)–(18) plus the so-called *marginal conditions*

$$\Lambda'(q(1)) = \frac{1}{\chi^2(q(1))}, \tag{27}$$

$$\Lambda'(q_1) = \frac{1}{\chi^2(q_1)}. \tag{28}$$

The dynamical solution leads, moreover, to the further identity

$$x(q_1) = p_1. \tag{29}$$

We notice that the solution is not overdetermined since, because of the presence of the continuous part in $q(x)$, Eq. (28) is not independent from Eq. (17).

The dynamic phase diagram is plotted in Fig. 7 where the static lines are also reported (dotted curves) for a direct comparison with the diagram of Fig. 2. As one can see, each static solution representing an equilibrium phase has its dynamic counterpart. The only difference is that the transition line between the F-1RSB and 1-F-1RSB phases can be both continuous (b) and discontinuous (a), whereas in the static case it was only continuous. The transition lines are, then, obtained from the dynamic solutions. In Table I we report, in the current notation for the overlap and the RSB parameter values, the description of all phases involved and the relative transitions.

Alternatively, one can determine the dynamic transitions starting from the analysis of the behavior of the static functions. The discriminating quantity is not the free energy, in this case, but the total complexity of the states[41,42] that is the average over the quenched disorder of the logarithm of the number of metastable states. Indeed, to see which phase is relevant at a given phase diagram point, one has to select the

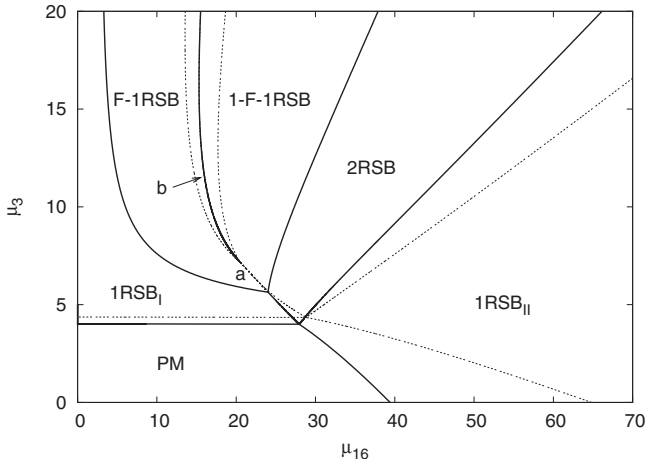

FIG. 7. Dynamic and static (dotted line) transition lines in the (μ_{16},μ_3) plane. The dynamic lines are all plotted as solid curves but for (a) (dashed line), which denotes the discontinuous part of the 1RSB$_I$-F-1RSB transition. By (b) we indicate the continuous part of this transition where statics and dynamics coincide.

one with the higher total complexity. Loci where the complexities of the different phases equal each other are, thus, the transition lines reported in Fig. 7. The complexity can be obtained, e.g., as the Legendre transform of the free energy Φ [cf. Eq. (3)] with respect to the parameter m—i.e., the last breaking point—corresponding to the *state level* in the ultrametric tree (see Fig. 5).

We eventually notice that, in Fig. 7, in one case the dynamic line coincides with the static one, at the F-1RSB/1-F-1RSB transition. This is typical of phase transitions where the $q(x)$ ends with a continuous part $[q(1)=q_c]$ on one side and with a discontinuous step on the other side of the transition line (that at $x=m$ in our notation). If the step is on top of a continuous part and goes to zero *smoothly*—that is, continuously—at the transition (as in the present case) or if a continuous part smoothly develops on top of the step (as is conjectured to occur in other models; see, e.g., Ref. 15), this implies that the complexity of the system goes to zero as well[43] and the dynamics does not get stuck at some excited state, thus reaching the thermodynamic static solution. The same is known to happen, e.g., in the $2+p$-spin version of the model[25,33] at the 1RSB-1-FRSB transition and in the Ising p-spin model[23,46] at the 1RSB-FRSB transition.

VI. CONCLUSION

In conclusion, developing the analysis of the $(s+p)$-spin spherical model with $s,p>2$ and large $p-s$, we find a very rich phase diagram with various candidate (mean-field) glassy phases, besides the usual 1RSB one. In a dynamic parallel, a RSB step is connected to a time-scale bifurcation of processes taking place in the glass former.[33,40] In the case of one- and two-step RSB's, we have, thus, phases with two or three kinds of processes active on separated time scales.

In solid glass formation, the main bifurcation is the one between the relaxation time of α processes, carrying structural relaxation and falling out of equilibrium at the glass transition (i.e., operatively speaking, when the viscosity of the glass former reaches the value of 10^{13} Poise), and the relaxation times of all faster (and equilibrated) β processes. The difference among the existing β processes is, usually, neglected in theoretical modeling, even though their relaxation times can differ for several orders of magnitude. The 2RSB phase might, then, describe systems where slow β (such as, e.g., Johari-Goldstein processes[47]) and fast β (e.g., collisions) processes are well separated. This is, indeed, what happens in many glasses where, at a temperature a few degrees below the glass transition temperature, Johari-Goldstein-like β relaxation occurs on time scales up to the order of a millisecond. This is much less than the α relaxation time (ca. 10^3 s) but about nine or ten orders of magnitude larger than the typical times of short-range collision of the molecules in the viscous liquid phase (the so-called *cage rattling*).

TABLE I. Dynamic transitions table. Looking at Fig. 7, the phases are ordered starting from the 1-F-1RSB one and spiraling counterclockwise around the quadricritical point. Notice that p_2 and q_2 in the 2RSB solution and p_1 and q_1 in the 1RSB solutions are equivalent notations to m and $q(1)$, respectively.

Solution	1-F-1RSB	F-1RSB	RSB$_I$	PM	1RSB$_{II}$	2RSB
1-F-1RSB		$m=1$ [a]				$q_c=q_1$
$[p_1,q_1,x_c,q_c,m,q(1)]$		$q(1)=q_c$ [b]				
F-1RSB	$m=1$ [a]		$q(1)=q_1$			
$[p_1,q_1,m,q(1)]$	$q(1)=q_c$ [b]					
1RSB$_I$		$q(1)=q_1$		$p_1=1$		$p_2=1$
$[p_1,q_1]$						
PM			$p_1=1$		$p_1=1$	
$[q(x)=0\forall x]$						
1RSB$_{II}$				$p_1=1$		$p_2=p_1$
$[p_1,q_1]$						
2RSB	$q_c=q_1$		$p_2=1$		$p_2=p_1$	
$[p_1,q_1,p_2,q_2]$						

In the framework of disordered systems theories, moreover, the existence of a thermodynamically consistent 2RSB phase opens the way to the study of the complexity contributions at the level of clusters of states, apart from the standard complexity of states, allowing for a probe of structures of metastable states in amorphous systems different from the known ones and including patterns that were conjectured before but never explicitly computed.[15,18]

Incidentally, we mention that adding more multibody interaction terms to the Hamiltonian, Eq. (1),

$$\mathcal{H} = \sum_{\alpha=1}^{R} \sum_{i_1<\cdots<i_{p_\alpha}} J_{i_1,\ldots,i_{p_\alpha}}^{(p_\alpha)} \sigma_{i_1} \cdots \sigma_{i_{p_\alpha}}, \tag{30}$$

one is able, in principle, to build a model presenting phases that are stable within a Parisi ansatz including any wanted number R of RSB's. Indeed, what matters is the shape of the function $[\Lambda'(q)]^{-1/2}$, the right-hand side of Eq. (13). More precisely, there is the possibility of finding, for certain, far apart, values of the numbers p_α of interacting spins, and in given regions of the external parameters space, a function $[\Lambda'(q)]^{-1/2}$ whose convexity in the interval $0<q<1$ changes sign a certain number of times. As we have seen, one change of convexity allows for the existence of a 2RSB phase. Two changes would signal the existence of a 3RSB phase and so forth.[48]

Eventually, the equivalence of the dynamic equations of spherical spin-glass models, in the PM phase, with the MC equations of schematic theories,[49] makes the $s+p$ model also an interesting instance of an off-equilibrium generalization of the MCT predictions below the MC transition, where the equivalence breaks down, since MCT assumes equilibrium (one Gibbs state). This would be relevant, above all, to deal with amorphous-to-amorphous transitions, in which both the interested phases are already frozen and, thus, equilibrium properties, such as, e.g., the fluctuation-dissipation theorem, cannot be taken for granted.

ACKNOWLEDGMENTS

We acknowledge V. Krakoviack and M. Müller for stimulating discussions.

*andrea.crisanti@roma1.infn.it
†luca.leuzzi@roma1.infn.it

[1] O. B. Tsiok, V. V. Brazhkin, A. G. Lyapin, and L. G. Khvostantsev, Phys. Rev. Lett. **80**, 999 (1998).
[2] L. Huang and J. Kieffer, Phys. Rev. B **69**, 224203 (2004).
[3] S. K. Deb, M. Wilding, M. Somayazulu, and P. F. McMillian, Nature (London) **414**, 528 (2001).
[4] O. Mishima, L. D. Calvert, and E. Walley, Nature (London) **314**, 74 (1985).
[5] P. H. Poole, F. Sciortino, U. Essmann, and H. E. Stanley, Nature (London) **360**, 324 (1992).
[6] S.-H. Chen, W.-R. Chen, and F. Mallamace, Science **300**, 619 (2003).
[7] D. Cangialosi, M. Wübbenhorst, H. Schut, A. van Veen, and S. J. Picken, J. Chem. Phys. **122**, 064702 (2005).
[8] F. Sciortino, Nat. Mater. **1**, 145 (2002).
[9] K. Dawson, G. Foffi, M. Fuchs, W. Götze, F. Sciortino, M. Sperl, P. Tartaglia, Th. Voigtmann, and E. Zaccarelli, Phys. Rev. E **63**, 011401 (2000).
[10] E. Zaccarelli, G. Foffi, K. A. Dawson, F. Sciortino, and P. Tartaglia, Phys. Rev. E **63**, 031501 (2001).
[11] A. Caiazzo, A. Coniglio, and M. Nicodemi, Phys. Rev. Lett. **93**, 215701 (2004).
[12] M. Mezard, G. Parisi, and M. A. Virasoro, *Spin Glass Theory and Beyond* (World Scientific, Singapore, 1987).
[13] D. J. Gross and M. Mezard, Nucl. Phys. B **240**, 431 (1984).
[14] E. Gardner, Nucl. Phys. B **257**, 747 (1985).
[15] D. J. Gross, I. Kanter, and H. Sompolinsky, Phys. Rev. Lett. **55**, 304 (1985).
[16] The solution is 1RSB below the critical temperature at which the paramagnetic phase ceases to be thermodynamically relevant, but above a second one ("Gardner temperature") below which it becomes inconsistent.
[17] A. Crisanti and H.-J. Sommers, Z. Phys. B: Condens. Matter **87**, 341 (1992).
[18] A. Montanari and F. Ricci-Tersenghi, Eur. Phys. J. B **33**, 339 (2003).
[19] R. Monasson, R. Zecchina, S. Kirkpatrick, B. Selman, and L. Troyansky, Nature (London) **400**, 133 (1999).
[20] A. Montanari, G. Parisi, and F. Ricci-Tersenghi, J. Phys. A **37**, 2073 (2004).
[21] D. Sherrington and S. Kirkpatrick, Phys. Rev. Lett. **35**, 1792 (1975).
[22] This is the conjecture of Ref. 15 for the Potts model and what seems to emerge from preliminary studies of the Ising p-spin model below the Gardner temperature (Ref. 23). As far as we know a thourough computation of the very-low-temperature phase of these models has yet to be performed.
[23] A. Crisanti and L. Leuzzi (unpublished).
[24] A. Crisanti and L. Leuzzi, Phys. Rev. Lett. **93**, 217203 (2004).
[25] A. Crisanti and L. Leuzzi, Phys. Rev. B **73**, 014412 (2006).
[26] Th. M. Nieuwenhuizen, Phys. Rev. Lett. **74**, 4289 (1995).
[27] V. Krakoviack, arXiv:0705.3187, Phys. Rev. B (to be published).
[28] W. Götze and L. Sjögren, J. Phys. C **20**, 879 (1986).
[29] W. Götze and L. Sjögren, J. Phys.: Condens. Matter **1**, 4183 (1989); **1**, 4203 (1989).
[30] V. Krakoviack, C. Alba-Simionesco, and M. Krauzman, J. Chem. Phys. **107**, 3417 (1997).
[31] V. Krakoviack and C. Alba-Simionesco, J. Chem. Phys. **117**, 2161 (2002).
[32] S. Ciuchi and A. Crisanti, Europhys. Lett. **49**, 754 (2000).
[33] A. Crisanti and L. Leuzzi, Phys. Rev. B **75**, 144301 (2007).
[34] For the expert reader we mention that the values of p corresponding to a certain s are lower than those provided by Krakoviack (Ref. 27). Those, indeed, correspond to the values of $p_d(s)$ for which the dynamic transition line between the paramagnetic phase and the frozen 1RSB phase develops a swallowtail. Some examples are $(s,p_d(s))=(3,10),(4,15.92),(5,21.79)$. Since the

swallowtail is a signal that the 1RSB is becoming unstable somewhere, it is a sufficient condition to have a p larger than or equal to p_d to know that more RSBs are needed. The appearence of the swallowtail is not, however, a necessary condition. To complete the picture, we also mention that a swallowtail develops in the static PM-1RSB transition line as well, at a still larger $p_s(s) > p_d(s)$. For instance, $(s, p_s(s)) = (3, 12.43), (4, 22.68), (5, 34.24)$.

[35] S. F. Edwards and P. W. Anderson, J. Phys. F: Met. Phys. **5**, 965 (1975).

[36] This kind of order parameter function was first conjectured for the lowest-temperature spin-glass phase of the mean-field disordered Potts model (Ref. 15).

[37] O. Rivoire, G. Biroli, O. C. Martin, and M. Mezard, Eur. Phys. J. B **37**, 55 (2004).

[38] This transition may occur, as well, if $x_1 \to 1$, but this does not take place in the present model.

[39] T. R. Kirkpatrick, D. Thirumalai, and P. G. Wolynes, Phys. Rev. A **40**, 1045 (1989).

[40] H. Sompolinsky, Phys. Rev. Lett. **47**, 935 (1981).

[41] A. Crisanti and H.-J. Sommers J. Phys. I **5**, 805 (1995).

[42] R. Monasson, Phys. Rev. Lett. **75**, 2847 (1995).

[43] We are speaking about the so-called BRST, or "supersymmetric," complexity counting states represented by minima of the free energy landscape; see Refs. 44 and 45 and references therein for a broadening on the subject.

[44] M. Müller, L. Leuzzi, and A. Crisanti, Phys. Rev. B **74**, 134431 (2006).

[45] G. Parisi, in *Computing the number of metastable states in infinite rage models*, Les Houches, Session LXXXIII, edited by A. Bovier, F. Dunlop, A. van Enter, F. Den Hollander, and J. Dalibard (Elsevier, Amsterdam, 2005).

[46] A. Crisanti, L. Leuzzi and T. Rizzo, Phys. Rev. B **71**, 094202 (2005).

[47] G. P. Johari and M. Goldstein, J. Chem. Phys. **55**, 4245 (1971).

[48] An example of a model with three multibody interaction terms is the one whose Langevin dynamics was studied in Ref. 11.

[49] For a review see J. P. Bouchaud, L. F. Cugliandolo, J. Kurchan, and M. Mezard, in *Spin Glasses and Random Fields*, edited by A. P. Young (World Scientific, Singapore, 1997).